



Vaasan yliopisto
UNIVERSITY OF VAASA

OSUVA Open
Science

This is a self-archived – parallel published version of this article in the publication archive of the University of Vaasa. It might differ from the original.

Energy management strategy in dynamic distribution network reconfiguration considering renewable energy resources and storage

Author(s): Azizivahed, Ali; Arefi, Ali; Ghavidel, Sahand; Shafie-khah, Miadreza; Li, Li; Zhang, Jiangfeng; Catalão, João P. S.

Title: Energy management strategy in dynamic distribution network reconfiguration considering renewable energy resources and storage

Year: 2020

Version: Final draft (post print, aam. accepted manuscript)

Copyright ©202X IEEE. Personal use of this material is permitted. Permission from IEEE must be obtained for all other uses, in any current or future media, including reprinting/republishing this material for advertising or promotional purposes, creating new collective works, for resale or redistribution to servers or lists, or reuse of any copyrighted component of this work in other works.

Please cite the original version:

Azizivahed, A., Arefi, A., Ghavidel, S., Shafie-khah, M., Li, L., Zhang, J., & Catalão, J.P. S., (2020). Energy management strategy in dynamic distribution network reconfiguration considering renewable energy resources and storage. *IEEE transactions on sustainable energy* 11(2), 662-673. <https://doi.org/10.1109/TSTE.2019.2901429>

Energy Management Strategy in Dynamic Distribution Network Reconfiguration considering Renewable Energy Resources and Storage

Ali Azizivahed, *Member, IEEE*, Ali Arefi, *Senior Member, IEEE*,
 Sahand Ghavidel, *Student Member, IEEE*, Miadreza Shafie-khah, *Senior Member, IEEE*,
 Li Li, *Member, IEEE*, João P. S. Catalão, *Senior Member, IEEE*, and Jiangfeng Zhang, *Member, IEEE*

Abstract—Penetration of renewable energy sources (RESs) and electrical energy storage (EES) systems in distribution systems is increasing, and it is crucial to investigate their impact on systems' operation scheme, reliability and security. In this paper, expected energy not supplied (EENS) and voltage stability index (VSI) of distribution networks are investigated in dynamic balanced and unbalanced distribution network reconfiguration, including RESs and EES systems. Furthermore, due to the high investment cost of the EES systems, the number of charge and discharge is limited, and the state-of-health constraint is included in the underlying problem to prolong the lifetime of these facilities. The optimal charging/discharging scheme for EES systems and optimal distribution network topology are presented in order to optimize the operational costs, and reliability and security indices simultaneously. The proposed strategy is applied to a large-scale 119-bus distribution test network in order to show the economic justification of the proposed approach.

Index Terms—Energy Management, Distribution Network Reconfiguration, Energy Storage, PV Panels, Reliability.

I. INTRODUCTION

OPERATIONAL strategies of distribution networks have significantly changed over the past decade due to the high penetration of renewable energy sources (RESs) and energy storages alongside automation systems [1]. The stochastic nature of RES poses a serious challenge to supply the demand in a reliable way. Accordingly, a lot of studies have been carried out to optimally manage charging and discharging schedules of energy storage units, which play a decisive role in the management of renewable energy sources within distribution networks [2-4]. In addition, as one of the prevalent techniques (due to the integration of automation

system in distribution networks), distribution feeder reconfiguration (DFR) is implemented on distribution systems in the presence of RES and energy storages. The DFR process is to apply changes to the topology of distribution networks in order to optimize certain objective functions subject to all operational constraints [5]. The DFR is carried out by managing the on/off states of tie-switches and sectionalizing-switches in a distribution feeder without islanding any buses.

The DFR problem can be formulated as a mixed-integer, non-linear and non-convex optimization problem. Therefore, traditional gradient based optimization algorithms are not suitable to solve DFR [6]. Accordingly, many researchers adopted intelligent evolutionary optimization methods to solve the distribution network reconfiguration problem. For example, in [7], an enhanced gravitational search algorithm is implemented to solve the DFR in order to improve transient stability and reduce operational cost and power losses. In [8], a hybrid evolutionary algorithm based on particle swarm optimization algorithm and Nelder–Mead simplex search algorithm is developed to minimize the active power loss. Furthermore, a modified genetic algorithm is proposed for DFR in [9] where the variable population size is taken into account. In [10], the optimal sizing, location, and network topology are obtained simultaneously by using optimal power flow to minimize operational cost and power losses.

Additionally, the deployment of RESs and electrical energy storages requires studies on the optimal management of these facilities. Many studies are carried out in order to obtain an optimal management scheme for electrical energy storages in the fixed-topology distribution networks. For instance, the optimal charging and discharging pattern for energy storage in the distribution network is obtained using a modified evolutionary algorithm to improve reliability and reduce operational cost [11]. In [12], technical and financial benefits of electrical energy storage systems in distribution networks are investigated. A dynamic model for the energy management of dispatchable distributed generation sources of micro-grids in the presence of wind farms and PV farms is formulated in [13] to balance the generation and demand. In [14], the energy storage units are allocated in optimal places in a distribution system integrated with wind power and PV sources in order to prolong the lifetime of energy storage units. Moreover, optimal investment cost of batteries is obtained in order to maximize the benefit [15].

This work was supported in part by International Science and Technology Cooperation Project of Sichuan Province, China, under Grant 2018HH0146. J.P.S. Catalão acknowledges the support by FEDER funds through COMPETE 2020 and by Portuguese funds through FCT, under SAICT-PAC/0004/2015 (POCI01-0145-FEDER-016434), 02/SAICT/2017 (POCI-01-0145-FEDER-029803) and UID/EEA/50014/2019 (POCI-01-0145-FEDER-006961).

A. Azizivahed, S. Ghavidel, L. Li and J. Zhang are with the Faculty of Engineering and Information Technology, University of Technology Sydney, PO Box 123, Broadway, NSW 2007, Australia (e-mails: {Sahand.GhavidelJirsaraie, Ali.Azizivahed}@student.uts.edu.au; {li.li, jiangfeng.zhang}@uts.edu.au).

A. Arefi is with the School of Engineering and Information Technology, Murdoch University, Perth, Australia. (email: a.arefi@murdoch.edu.au).

M. Shafie-khah is with School of Technology and Innovations, University of Vaasa, 65200 Vaasa, Finland (e-mail: mshafiek@univaasa.fi).

J.P.S. Catalão is with INESC TEC and the Faculty of Engineering of the University of Porto, Porto 4200-465, Portugal (e-mail: catalao@fe.up.pt).

It is noteworthy that the above-mentioned literature regarding DFR has ignored the daily load variation and solved the DFR during a predetermined time interval. The DFR model for non-variable loads cannot demonstrate the real scenarios and cannot achieve the optimal solution for 24-hour time scheduling for variable load distribution networks. To fill this gap, the DFR is determined in [16] for different time horizons (year, season, month and day) in order to find the most optimal switching cost. In [17], the DFR is applied to an unbalanced distribution network over a 24-hour time horizon. In addition, genetic algorithm is implemented as an optimization tool for minimizing network energy losses. Though the presented robust strategy in [17] considers the uncertain price, load consumption and RES power generation are treated deterministically based on a fixed prediction. In a distribution system with high penetration of RESs, applying stochastic programming in order to model intermittent behavior of these uncertainty sources is a prevalent and practical solution for distribution operations. In addition, the solution for dynamic DFR in the presence of RESs integrated with energy storages is not evaluated markedly in the aforementioned literature.

Accordingly, an improved optimization model is expected to include these three aspects: dynamic distribution feeder reconfiguration, optimal management scheme for energy storages integrated with RESs, and meeting demand in a reliable and stable way considering uncertainties in RESs power generation, energy price and load consumption. The mentioned model should give operators a decision-making strategy in which the most suitable DFR is achieved by proper DG unit dispatching pattern, optimal energy storage charging/discharging control, and appropriate reliability and stability levels. Eventually, the problem can be completed when the constraints related to the technical and operational aspects are considered through DFR and energy management problem. To address the above-mentioned problem, this paper presents reliability and stability oriented management scheme. The main contributions of this paper are summarized as follows.

- The dynamic distribution networks and energy management are modeled simultaneously. The obtained results include optimal switching plan, optimal batteries charging/discharging schedule and optimal daily diesel generators dispatching.
- The energy not supplied is considered as a separate objective function based on graph theory. Similarly, the voltage stability based on the distribution network loadability is formulated.
- Scenario reduction strategy and shuffled frog leaping algorithm (SFLA) are utilized in order to obtain the optimal solutions for both balanced and unbalanced distribution networks. Also, the intermittent nature of electricity price, load consumption and PV generations are considered as uncertainty sources.

The remainder of this paper is organized as follows. Section II presents the underlying problem formulation and framework. It consists of decision variables, objective functions, problem constraints and optimization methodology. Section III presents case studies and numerical results, and finally, Section IV concludes the paper.

II. PROBLEM DEFINITION AND FRAMEWORK

In some cases, DISCO is the owner of some parts of distribution network [18]. Here, it is assumed that only one DISCO is the owner of all facilities and operates the distribution network. It solves the stochastic optimization problem by considering uncertainty in PV generation and electricity price. The problem formulation is explained in the following six parts; decision variables, objective functions (operational cost, reliability index and security index), operational limitations and constraints, and uncertainty modeling and optimization tool.

A. Decision Variables

The decision variables of underlying problem include graph topology of the network, diesel generators active power and batteries charge and discharge scheme as follows:

$$\mathbf{X} = [\mathbf{X}_{Sw} \quad \mathbf{X}_{DG} \quad \mathbf{X}_{Batt} \quad \mathbf{X}_{Tap}] \quad (1)$$

$$\mathbf{X}_{Sw} = [\bar{X}_{Sw_1} \quad \bar{X}_{Sw_2} \quad \dots \quad \bar{X}_{Sw_{Nsw}}] \quad (2)$$

$$\mathbf{X}_{DG} = [\bar{X}_{DG_1} \quad \bar{X}_{DG_2} \quad \dots \quad \bar{X}_{DG_{NDG}}] \quad (3)$$

$$\mathbf{X}_{Batt} = [\bar{X}_{Batt_1} \quad \bar{X}_{Batt_2} \quad \dots \quad \bar{X}_{Batt_{NBatt}}] \quad (4)$$

$$\mathbf{X}_{Tap} = [\bar{X}_{Tap_1} \quad \bar{X}_{Tap_2} \quad \dots \quad \bar{X}_{Tap_{NTap}}] \quad (5)$$

$$\bar{X}_{Sw_k} = [X_{Sw_k}^1 \quad X_{Sw_k}^2 \quad \dots \quad X_{Sw_k}^{24}], \quad k \in \{1, 2, \dots, Nsw\} \quad (6)$$

$$\bar{X}_{DG_k} = [X_{DG_k}^1 \quad X_{DG_k}^2 \quad \dots \quad X_{DG_k}^{24}], \quad k \in \{1, 2, \dots, NDG\} \quad (7)$$

$$\bar{X}_{Batt_k} = [X_{Batt_k}^1 \quad X_{Batt_k}^2 \quad \dots \quad X_{Batt_k}^{24}], \quad k \in \{1, 2, \dots, NBatt\} \quad (8)$$

$$\bar{X}_{Tap_k} = [X_{Tap_k}^1 \quad X_{Tap_k}^2 \quad \dots \quad X_{Tap_k}^{24}], \quad k \in \{1, 2, \dots, NTap\} \quad (9)$$

where, \mathbf{X} is the decision variable vector of the proposed problem which consists of four sub-decision variables: open switches (\mathbf{X}_{Sw}), diesel generators output (\mathbf{X}_{DG}), batteries active power charge/discharge (\mathbf{X}_{Batt}) and tap position of the tap-changer (\mathbf{X}_{Tap}). Notations \bar{X}_{Sw_k} , \bar{X}_{DG_k} , \bar{X}_{Batt_k} and \bar{X}_{Tap_k} are the k^{th} set of open switch numbers, active power output of k^{th} diesel generator, active power of charge/discharge of the k^{th} battery, and tap position of the k^{th} tap-changer, at a 24-hour time horizon, respectively.

B. Operational Cost

The operational cost includes the cost of energy purchasing from substation, the fuel cost of diesel generators and switching which can be formulated as:

$$\begin{aligned} Cost = & \sum_{t=1}^{24} \sum_{s=1}^{N_s} \rho_s \left(\sum_{n=1}^{N_{Sub}} C_{n,t,s}^{SS} \times P_{n,t,s}^{SS} + \sum_{j=1}^{N_{DG}} C_{j,t,s}^{DG} \times P_{j,t,s}^{DG} \right) \\ & + \sum_{t=1}^{24} \sum_{k=1}^{N_{Sw}} C^{Sw} \times |S_k^t - S_{0,k}^t| \end{aligned} \quad (10)$$

where, $C_{n,t,s}^{SS}$, $C_{j,t,s}^{DG}$ and C^{Sw} are the price of energy from n^{th} substation at t^{th} time interval for s^{th} scenario, the price of fuel of j^{th} diesel generator at t^{th} time interval for s^{th} scenario and switching cost, respectively; ρ_s is the probability of s^{th} scenario; N_{Sub} (N_{DG}) and N_{Sw} are the number of substations (diesel generators) and the number of switches, respectively;

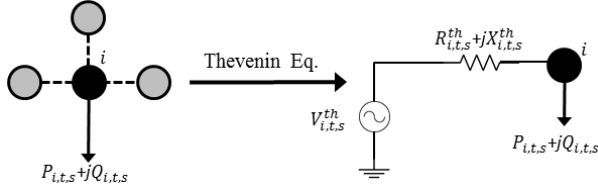


Fig. 1. Thevenin equivalent system of bus i at t^{th} hour for s^{th} scenario

N_s is the number of scenarios; $P_{n,t,s}^{SS}$ and $P_{j,t,s}^{DG}$ are the active power from n^{th} substation and active power from j^{th} diesel generator at t^{th} time interval for s^{th} scenario, respectively; and S_k^t and $S_{0,k}^t$ are the new and initial status of k^{th} switch at t^{th} time interval.

C. Desire Reliability Index

Almost all power outages and blackouts are caused by faults in the transmission and distribution networks [19, 20]. Accordingly, the operational problems should be carried out to optimize a reliability index such as minimization of EENS as follows:

$$EENS = \sum_{t=1}^{24} \sum_{i=2}^{N_{bus}} EENS_{i,t}, \quad (11)$$

where, $EENS_i^t$ is the expected energy not supplied of i^{th} bus at t^{th} time interval; and N_{bus} is the number of buses. Notation $EENS_{i,t}$ is defined as follows:

$$EENS_{i,t} = \sum_{s=1}^{N_s} \rho_s P_{i,t,s} \times \left(\sum_{l \in H_i} U_l + \sum_{k \in H'_i} U'_k \right), \quad (12)$$

where, $P_{i,t,s}$ is the total generation and consumption of active power of i^{th} bus at t^{th} time interval for s^{th} scenario; H_i and H'_i are the set of downstream and upstream branches of i^{th} bus, respectively; U_l and U'_k are the service unavailability related to the repair time of l^{th} downward branch of the i^{th} bus and the service unavailability associated to the restoration time of k^{th} upward branch of the i^{th} bus, respectively. Notations U_l and U'_k are defined as follows:

$$\begin{aligned} U_l &= \beta_l \times t_l \\ U'_k &= \beta_k \times t'_k \end{aligned} \quad (13)$$

where, β_l and β_k are the failure rate (fail/year) of l^{th} and k^{th} branch, respectively; and t_l and t'_k are the average reparation of l^{th} branch and restoration time of k^{th} branch, respectively.

D. Voltage Stability Index

Voltage collapse is one of the negative consequences of increasing load in distribution systems. In order to improve the network loadability, the voltage stability index is included in the underlying problem and defined based on ‘‘Thevenin-equivalent’’ [21]. The advantage of this strategy in comparison with the previous methods in [22] is that it can be implemented on both mesh and radial networks. More details of this method are explained as follows.

First, the Thevenin-equivalent will be obtained for all bases of networks as shown in **Error! Reference source not found.**

According to the load flow technique, (14) and (15) can be obtained; and from these equations, (16) can be obtained [22].

$$I_{i,t,s} = \frac{V_{i,t,s}^{th} - V_{i,t,s}}{R_{i,t,s}^{th} + jX_{i,t,s}^{th}} \quad (14)$$

$$P_{i,t,s} - jQ_{i,t,s} = V_{i,t,s}^* \times I_{i,t,s} \quad (15)$$

$$P_{i,t,s} - jQ_{i,t,s} = V_{i,t,s}^* \times \frac{V_{i,t,s}^{th} - V_{i,t,s}}{R_{i,t,s}^{th} + jX_{i,t,s}^{th}} \quad (16)$$

Eq. (17) can be calculated from (16). Coefficients $B_{i,t,s}$ and $C_{i,t,s}$ are defined by (18) and (19), respectively.

$$|V_{i,t,s}|^4 - B_{i,t,s} |V_{i,t,s}|^2 + C_{i,t,s} = 0 \quad (17)$$

$$B_{i,t,s} = |V_{i,t,s}^{th}|^2 - 2P_{i,t,s} R_{i,t,s}^{th} - 2Q_{i,t,s} X_{i,t,s}^{th} \quad (18)$$

$$C_{i,t,s} = (P_{i,t,s}^2 + Q_{i,t,s}^2) \cdot \left((R_{i,t,s}^{th})^2 + (X_{i,t,s}^{th})^2 \right) \quad (19)$$

In order to have a stable condition, constraint (20) is required. Therefore, the VSI will be defined as in (21).

$$B_{i,t,s}^2 - 4C_{i,t,s} \geq 0 \quad (20)$$

$$\begin{aligned} vsi_{i,t,s} &= \left(|V_{i,t,s}^{th}|^2 - 2P_{i,t,s} R_{i,t,s}^{th} - 2Q_{i,t,s} X_{i,t,s}^{th} \right)^2 - \\ &4 \cdot (P_{i,t,s}^2 + Q_{i,t,s}^2) \cdot \left((R_{i,t,s}^{th})^2 + (X_{i,t,s}^{th})^2 \right) \\ i &= 2, 3, \dots, N_{bus} \end{aligned} \quad (21)$$

All parameters in (14)-(21) are depicted in **Error! Reference source not found.** In order to reach a stable operation condition, VSI for all buses must be greater than zero. In this regard, the third objective function is defined as follow;

$$vsi_{i,t,s} = [vsi_{2,t,s}, vsi_{3,t,s}, \dots, vsi_{N_{bus},t,s}] \quad (22)$$

$$bvs_i_{i,t,s} = \begin{cases} 0 & vsi_{i,t,s} > 0 \\ 1 & vsi_{i,t,s} \leq 0 \end{cases} \quad (23)$$

$$Bvsi_{i,t,s} = [bvs_i_{2,t,s}, bvs_i_{3,t,s}, \dots, bvs_i_{N_{bus},t,s}] \quad (24)$$

$$penalty\ factor = \mathcal{M} \times \text{sum}(Bvsi_{i,t,s}) \quad (25)$$

$$VSI_{t,s} = \frac{1}{\min(vsi_{i,t,s})} + penalty\ factor \quad (26)$$

$$VSI = \frac{1}{24} \sum_{t=1}^{24} \sum_{s=1}^{N_s} \rho_s VSI_{t,s} \quad (27)$$

VSI is the third objective function. The parameter \mathcal{M} is a large number (for instance, 10^{100}) which is used as a penalty factor. The penalty factor is implemented to eliminate the unstable decision variables during the optimization process.

E. Technical and Operational Constraints

In this section, all the relevant technical and operational constraints are explained as below.

- *Distribution network radial structure*

Almost all distribution networks are operated in radial topology in order to simplify the protection systems. In order to satisfy the radial structure constraint, the bus branch incidence matrix is implemented. More details regarding the proposed matrix can be found in [23].

- *Diesel generator limitation*

As mentioned, the proposed problem is solved dynamically. In this regard, the ramp rate constraints should be considered besides the maximum and minimum output limitations.

$$P_j^{DG,min} \leq P_{j,t,s}^{DG} \leq P_j^{DG,max} \quad \forall j, t, s, \quad (28)$$

$$Ramp_j^{Down} \leq P_{j,t,s}^{DG} - P_{j,t-1,s}^{DG} \leq Ramp_j^{Up} \quad \forall j, t, s, \quad (29)$$

where, $P_j^{DG,min}$ and $P_j^{DG,max}$ are the minimum and maximum limitations of j^{th} diesel generator, respectively; and $Ramp_j^{Down}$ and $Ramp_j^{Up}$ are down and up ramp rates of j^{th} diesel generator, respectively.

- *Current and voltage limitations*

The bus voltages and branch currents should be within their maximum and minimum boundaries.

$$SL_{j,t,s} \leq SL_j^{max} \quad (30)$$

$$V_k^{min} \leq V_{k,t,s} \leq V_k^{max} \quad (31)$$

where $SL_{j,t,s}$ and SL_j^{max} are the power flow magnitude of j^{th} branch at t^{th} hour for s^{th} scenario and its corresponding maximum power flow limitation, respectively; and V_k^{min} and V_k^{max} are the minimum and maximum voltage of k^{th} bus.

- *Battery constraints*

Because of the high investment cost of energy storages, they should be operated in a secure environment to prolong their lifetime. In this regard, the maximum permitted number of switching back and forth between charging and discharging status must be considered besides the state of charge and other constraints.

$$E_{i,t} = E_{i,t-1} + \rho_{ch,i} \times P_{ch,i,t} \times \Delta t - \frac{1}{\rho_{dis,i}} P_{dis,i,t} \times \Delta t, \quad (32)$$

$$i = 1, 2, \dots, NBatt, \quad t = 1, \dots, 24, \quad \Delta t = 1h$$

$$E_i^{min} \leq E_{i,t} \leq E_i^{max}, \quad i = 1, 2, \dots, NBatt \quad t = 1, \dots, 24 \quad (33)$$

$$P_{ch,i,t} \leq P_{ch,i}^{max}, \quad i = 1, 2, \dots, NBatt, \quad t = 1, \dots, 24 \quad (34)$$

$$P_{dis,i,t} \leq P_{dis,i}^{max}, \quad i = 1, 2, \dots, NBatt, \quad t = 1, \dots, 24 \quad (35)$$

$$\sum_{t=1}^{23} |S_{t+1} - S_t| / 2 \leq N_{CH/DCH} \quad (36)$$

where $E_{i,t}$ is the amount of energy storage in the i^{th} battery at t^{th} hour. $P_{ch,i,t}$ ($P_{dis,i,t}$) is the permitted rate of charge (discharge) of i^{th} battery during a determinate period of time ($\Delta t = 1h$). $\rho_{ch,i}$ ($\rho_{dis,i}$) is the charge (discharge) efficiency percentage of the i^{th} battery. E_i^{max} (E_i^{min}) is the maximum (minimum) amount of permitted energy storage in i^{th} battery. Constraints (34) and (35) impose the maximum charge rate $P_{ch,i}^{max}$, and maximum discharge rate, $P_{dis,i}^{max}$, of the i^{th} battery during a determinate period of time ($\Delta t = 1h$). In constraint (36), $N_{CH/DCH}$ is the maximum permitted number of switching back and forth between charging and discharging status and S_t represents the charging and discharging status which is equal to 1 and -1 for charging and discharging status, respectively.

F. Uncertainty Characterization

In this study, two sources of uncertainty are considered.

- Electricity price of power supplied by substation
- Output power of PV plants.

1) *PV power uncertainty modeling*: For each time period,

historical data of solar irradiance are used to produce a beta [24] distribution function as follows;

$$f_b(s) = \begin{cases} \frac{\Gamma(\alpha + \beta)}{\Gamma(\alpha) \cdot \Gamma(\beta)} \cdot s^{(\alpha-1)} \cdot (1-s)^{(\beta-1)}, & 0 \leq s \leq 1 \\ & \alpha, \beta \geq 0 \\ 0, & \text{Otherwise} \end{cases} \quad (37)$$

where $f_b(s)$ is the beta distribution function. α and β are the parameters of the beta distribution function and can be obtained using historical data.

The continuous hourly beta PDFs are split into several intervals with equal width. Each interval has a mean value and a probability of occurrence which can be calculated as follows.

$$\rho_i^s = \int_{s_i}^{s_{i+1}} f_b(s) ds_i \quad (38)$$

where s_i and s_{i+1} indicate the starting and ending points of the interval i , respectively.

The output power of a PV plant corresponding to specific solar irradiation can be calculated as follows.

$$P_{y,t}^S(s_{y,t}) = N \times FF \times V_{y,t} \times I_{y,t} \quad (39)$$

$$FF = \frac{V_{MPP} \times I_{MPP}}{V_{oc} \times I_{sc}} \quad (40)$$

$$V_{y,t} = V_{oc} - K_v \times T_{y,t}^c \quad (41)$$

$$I_{y,t} = s_{y,t} [I_{sc} - K_i \times (T_{y,t}^c - 25)] \quad (42)$$

$$T_{y,t}^c = T_A + s_{y,t} \left(\frac{N_{OT} - 20}{0.8} \right) \quad (43)$$

where $T_{y,t}^c$ is cell temperature ($^{\circ}C$); T_A is ambient temperature ($^{\circ}C$); K_v and K_i are voltage and current temperature coefficient ($V/^{\circ}C$ and $A/^{\circ}C$), respectively; N_{ot} denotes nominal operating temperature of cell ($^{\circ}C$); FF is fill factor; I_{sc} and V_{oc} indicates short circuit current and open circuit voltage (A and V), respectively; I_{MPP} and V_{MPP} are, respectively current and voltage at maximum power point (A and V); $P_{y,t}^S$ is output power of the PV module; $s_{y,t}$ solar irradiance; and t and y are the indices of time periods and scenarios.

2) *Market prices uncertainty modeling*: In this paper, log-normal distribution function [25] is considered to characterize the market price of each hour. Accordingly, the market prices can be expressed as follows;

$$f_p(E^{pr}, \mu, \sigma) = \frac{1}{E^{pr} \sigma \sqrt{2\pi}} \exp\left(-\frac{(\ln E^{pr} - \mu)^2}{2\sigma^2}\right) \quad (44)$$

where μ and σ represent mean value and standard deviation, respectively, and E^{pr} is the distribution function parameter (i.e., electricity market price).

In a similar way, the log-normal PDFs are sliced into several intervals. Each interval yields a mean value and

probability of occurrence.

Different realization of PV power production and market prices can be modeled using a scenario generation process according to roulette wheel mechanism [26].

In this method, a large number of scenarios is generated. Higher numbers of scenarios result in a more precise modeling of the system. However, the higher number of scenarios causes higher computational burden. To this end, the number of scenarios should be selected in a way that not only diminishes the computational burden of the problem but also maintains a good approximation of the uncertain parameters. In order to reduce the number of scenarios and consequently reduce the computational time; the backward method is implemented to eliminate the duplicate scenarios or the scenarios with minimum distance [27].

G. Multi-objective Strategy and Optimization Tool

In this section, the multi-objective technique and the shuffled frog leaping algorithm (SFLA) are introduced. The **ALGORITHM** and Fig. 2 describe the proposed multi-objective technique. According to this method, all populations are sorted in ascending order of the first objective function, then an eliminating zone is defined for each individual (i.e. Fig. 2), and based on that, some populations are eliminated. This process is applied to reach a set of non-dominated solutions.

The ranges of objective function values are different in the multi-objective programming. Therefore, the fuzzy decision-making technique (i.e. based on trapezoidal fuzzy membership functions) is employed in order to have the same range for all of them.

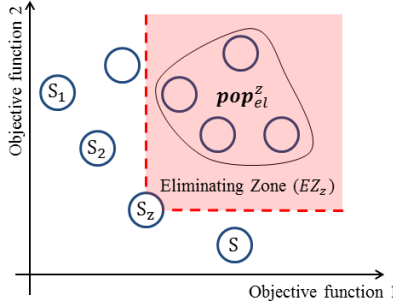


Fig. 2. Eliminating zone for each solution

ALGORITHM

1. **Input:** $pop = [population \ \& \ objective \ functions]$.
2. **Sort** the population in ascending order of the first objective function.
3. $z=1, N_{pop} = \text{number of population}$.
4. **While** $z \leq N_{pop}$
5. Constitute the eliminating zone (EZ_z) for z^{th} population (red shadow in Fig. 2).
6. Eliminate the populations that are in the eliminating zone of z^{th} population.
 $pop_{el}^z \subseteq pop$ &
 $pop_{el}^z = \{set \ of \ populations \ in \ the \ EZ_z \ area\}$
 $pop = pop \setminus \{pop_{el}^z\}$
7. Update $z=z+1, N_{pop} = \text{number of population}$.
8. **end**
9. **Output:** set of non dominated solutions = pop .

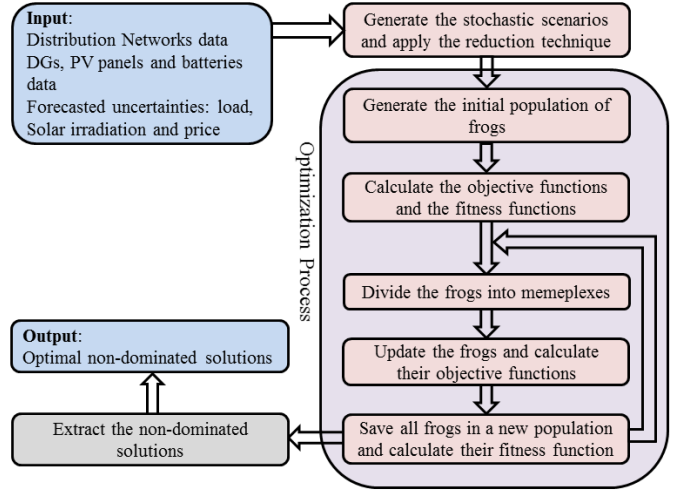


Fig. 3. The optimization framework of energy management and distribution network reconfiguration

$$\mu_{Obj_m}(X) = \begin{cases} 1 & Obj_m \leq Obj_m^{min} \\ \frac{Obj_m^{max} - Obj_m}{Obj_m^{max} - Obj_m^{min}} & Obj_m^{min} \leq Obj_m \leq Obj_m^{max} \\ 0 & Obj_m \geq Obj_m^{max} \end{cases} \quad (45)$$

where Obj_m and Obj_m^{max} (Obj_m^{min}) are the m^{th} objective function and its corresponding upper (lower) bound, respectively, and μ_{Obj_m} is the fuzzy set for m^{th} objective function.

The fitness function is determined for each individual as follows:

$$\varphi_i = \frac{\sum_{m=1}^{N_{Obj}} \omega_m \times \mu_{Obj_m}(X_i)}{\sum_{k=1}^{N_{nd}} \sum_{m=1}^{N_{Obj}} \omega_m \times \mu_{Obj_m}(X_i)} \quad (46)$$

where N_{nd} is the number of non-dominated solution; φ_i and ω_m are the fitness function of i^{th} non-dominated solution and the weighting factor (i.e. the priority grade from the decision makers point of view) of m^{th} objective function, respectively. In this study, $\omega_1 = \omega_2 = \omega_3 = 0.33$ is chosen.

SFLA is implemented to solve the above optimization problem. This algorithm models the social life of group of frogs when they are searching food. The details of this method are available in [28].

The frogs are divided equally into several memeplexes. In this algorithm, the worst frog (X_{worst}) in each memeplex is updated according to two strategies based on the best frog in the memeplex (X_{best}) and the best frog in all population (X_{Gbest}) as follows;

$$X_{worst}^{new} = X_{worst} + rand \times (X_{best} - X_{worst}) \quad (47)$$

$$X_{worst}^{new} = X_{worst} + rand \times (X_{Gbest} - X_{worst}) \quad (48)$$

where $rand$ is random number between 0 and 1. In the optimization process, the worst frog is updated by the best frog in the memeplex as in (47). If the fitness function for X_{worst}^{new} is better than of X_{worst} , then X_{worst} will be replaced by X_{worst}^{new} ; otherwise X_{worst} will be updated by the best frog in all population as in (48). Similarly, if the fitness function for X_{worst}^{new} is better than X_{worst} , X_{worst} will be replaced by X_{worst}^{new} , and if not, X_{worst} will be replaced by a new randomly generated frog.

This process will be applied for all memplexes and for a predetermined number of iterations. The framework of the proposed strategy is depicted in **Error! Reference source not found.**

III. SYSTEM MODEL AND SIMULATION RESULTS

In order to assess the performance of the proposed method, a case study based on the 119-bus distribution network is provided in this section.

A. Case Study

The 119-bus distribution network under study is shown in Fig. 4(a), consisting of three feeders, 15 tie-switches and 11 kV substation [29]. The average hourly forecasted active and reactive load profile is shown in Fig. 4(b). Four 500 kW PV panels and their relevant batteries are installed at bus#31, bus#42, bus#96 and bus#109. Five 500 kW diesel generators with unit power factor and 50 kW/h up and down ramp rate are located at bus#20, bus#28, bus#71, bus#74 and bus#111. 30 scenarios are implemented in order to simulate the uncertainty parameters. The simulation is done in MATLAB R2011b environment using a core-i5 processor laptop with 2.4 GHz clock frequency and 4.0 GB of RAM.

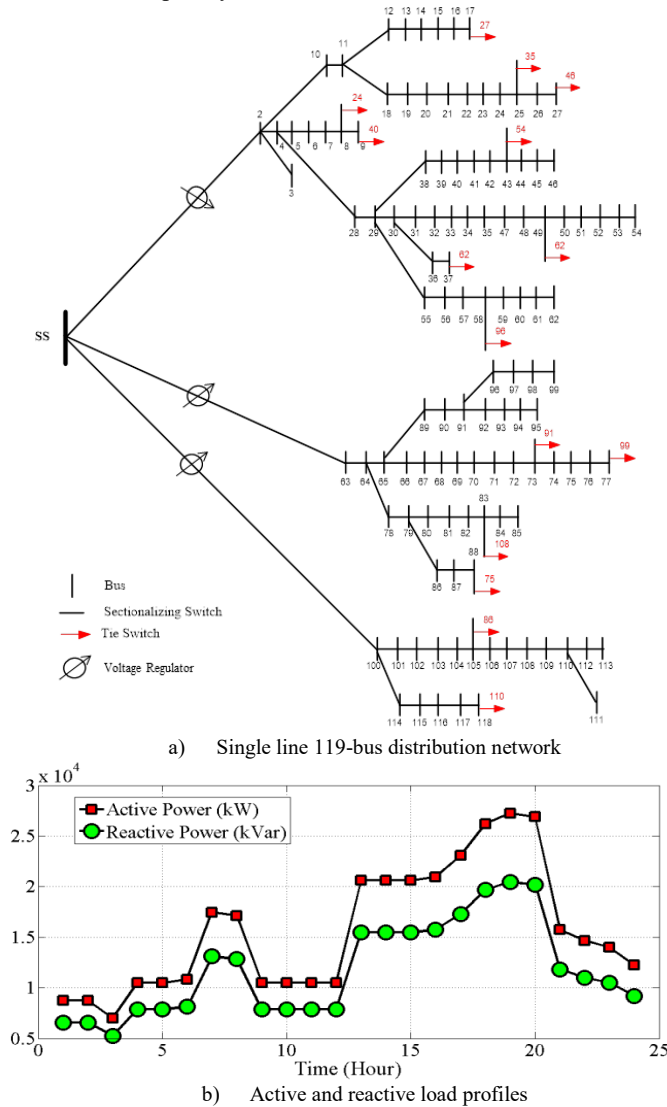


Fig. 4. Data for 119-bus standard distribution system

TABLE I
RESULTS OF DIFFERENT METHOD FOR MINIMIZING THE OPERATIONAL COST

Method	Operational Cost (\$)				
	Best	Mean	Worst	STD	C.T.
GA	13068.06	13206.7	13355.0	109.81	201
PSO	12835.64	12985.2	13355.0	212.32	164
DE	12835.64	12903.5	13161.1	99.79	178
SFLA	12820.85	12841.2	12897.1	25.32	167

C.T.: Computational Time (Second)

B. Simulation and Results

The three objective functions (Eqs. 10, 12 and 27) are important for the reliable and cost-effective operation of the distribution system; however, it is usually impossible to achieve the optimal results for all of them simultaneously. Also, the operation of diesel generators, batteries, and network switches are different in each case. Hence, various analyses are performed to explore the best compromise solution as will be described in the following.

1) *Single objective case study*: SFLA is compared with three different heuristic methods such as genetic algorithm (GA), particle swarm optimization (PSO) and differential evolution (DE), each is run 10 times to solve the DFR optimization problem, and the comparison results are detailed in **Error! Reference source not found.** Although the PSO reaches the optimal solution in a slightly shorter computational time compared to the SFLA, the obtained results by the SFLA are better than those obtained by the other methods. And also, it has a more robust performance than other algorithms. Therefore, in the following, only SFLA is used.

TABLE II shows the results of the optimization results for individual objectives and the initial condition (distribution network without DG units, PV panels and energy storages). Firstly, it is worth mentioning that the objective values of all objective functions are improved due to the positive impact of these facilities. In addition, the targeted objective (for example, operational cost) is minimized, and subsequently, the values of the other two objectives are calculated in each case. According to this table, the amount of optimal operational cost, optimal EENS, and optimal VSI are \$12820.85, 340.73 kWh/year and 2.53 p.u., respectively. Also, it can be seen that the operational cost is sharply in conflict with two other objective functions. In other words, by minimizing operational cost, the amount of ENS and VSI are increased (368.646 kWh/year and 3.397 p.u.). And similarly, by minimizing the ENS and VSI, the amount of operational cost is increased to \$13413.68 and \$12939.96, respectively. Similarly, the operational cost conflicts with VSI. The optimal VSI amount is 2.1, and in this condition, the amount of operational cost is \$13278.1.

The list of open-switches for minimizing operational cost is shown in 0. it is worth mentioning that the radiality constraint is satisfied in each hour. furthermore, Fig. 5 and Fig. 6 show the diesel generators active power output and batteries active power charge/discharge. as can be seen, almost all the diesel generators are operated at their minimum level in order to minimize the operational cost. also, from Fig. 6 it can be seen that the maximum permitted number of switching back and

forth between the charging and discharging status and the charging and discharging status constraint are satisfied for all batteries.

The list of open-switches for minimizing operational cost is shown in 0. It is worth mentioning that the radiality constraint is satisfied in each hour. Furthermore, Fig. 5 and Fig. 6 show the diesel generators active power output and batteries active power charge/discharge. As can be seen, almost all the diesel generators are operated at their minimum level in order to minimize the operational cost. Also, from Fig. 6 it can be seen that the maximum permitted number of switching back and forth between the charging and discharging status and the charging and discharging status constraint are satisfied for all batteries.

TABLE II
RESULTS OF MINIMIZING THE OBJECTIVE FUNCTIONS SEPARATELY

Method	Cost (\$)	ENS (kWh/year)	VSI (p.u.)
Initial Condition	15633.87	544.7785	4.0509
Cost Minimization	12820.85	368.646	3.3974
ENS Minimization	13413.68	340.7324	3.3831
VSI Minimization	12939.96	367.9338	2.5336

TABLE III
LIST OF OPEN SWITCHES FOR MINIMIZING OPERATIONAL COST

Hour	Open Switches
1	43-11- 23- 51- 47- 61- 38- 56- 72- 73- 98- 82- 85- 131- 32
2	45- 12- 17- 53- 122- 36- 39- 57- 66- 73- 128- 105- 101- 115- 33
3	43- 24- 20- 53- 46- 36- 27- 54- 71- 127- 98- 105- 102- 116- 33
4	43- 12- 120- 52- 48- 123- 27- 56- 126- 127- 96- 81- 102- 115- 33
5	118- 16- 7- 50- 48- 61- 124- 55- 70- 127- 76- 106- 101- 131- 34
6	42- 25- 120- 51- 48- 123- 38- 55- 71- 87- 128- 105- 103- 113- 34
7	118- 14- 23- 49- 46- 36- 37- 57- 89- 127- 128- 105- 103- 115- 32
8	44- 12- 120- 121- 48- 61- 37- 56- 66- 127- 76- 82- 85- 108- 132
9	118- 14- 23- 53- 122- 61- 39- 57- 68- 73- 75- 105- 103- 109- 33
10	44- 24- 21- 53- 47- 58- 37- 56- 72- 74- 96- 129- 130- 131- 31
11	41- 13- 23- 53- 122- 59- 38- 125- 70- 87- 96- 82- 102- 113- 30
12	45- 15- 19- 52- 48- 58- 124- 57- 89- 87- 97- 129- 85- 108- 34
13	41- 12- 23- 50- 47- 36- 124- 57- 70- 87- 76- 105- 85- 115- 31
14	41- 16- 17- 121- 48- 58- 39- 57- 126- 87- 128- 81- 85- 116- 34
15	118- 14- 120- 50- 46- 58- 38- 56- 88- 74- 128- 105- 102- 116- 34
16	42- 14- 20- 52- 122- 123- 124- 55- 72- 127- 97- 105- 103- 117- 33
17	42- 12- 23- 49- 48- 61- 39- 56- 71- 74- 76- 80- 100- 116- 34
18	45- 15- 18- 121- 48- 58- 124- 57- 71- 73- 128- 81- 102- 116- 34
19	45- 15- 20- 51- 48- 36- 124- 57- 72- 87- 128- 105- 85- 109- 30
20	45- 16- 7- 50- 122- 58- 27- 54- 71- 86- 97- 82- 103- 109- 30
21	41- 10- 18- 121- 122- 58- 38- 57- 90- 127- 96- 106- 101- 108- 33
22	43- 14- 21- 51- 46- 60- 38- 57- 72- 127- 97- 81- 85- 115- 34
23	43- 25- 22- 121- 47- 58- 39- 54- 69- 86- 75- 82- 100- 114- 34
24	118- 14- 120- 53- 48- 58- 124- 54- 68- 87- 76- 106- 103- 109- 33

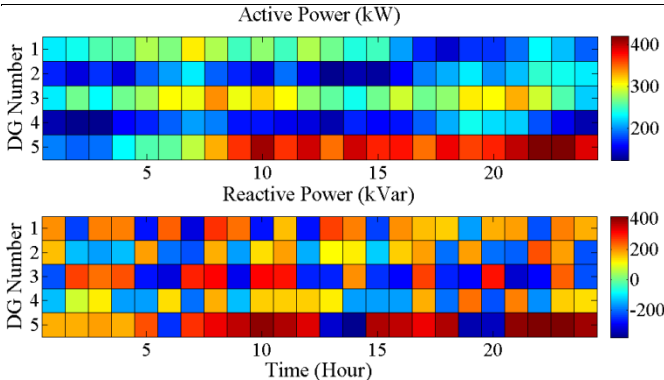


Fig. 5. Diesel generator power scheduling for the optimal operational cost.

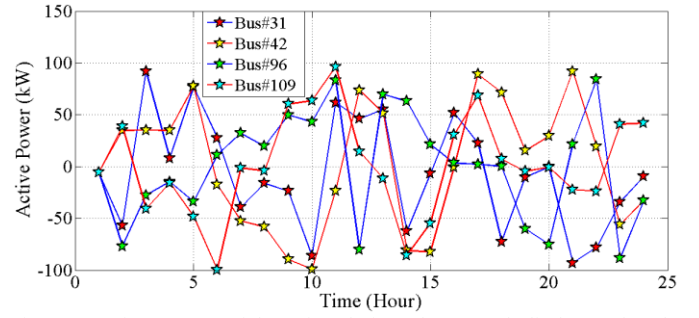


Fig. 6. Active power of batteries during charge and discharge for the optimal operational cost.

2) *Multi-objective case study:* As mentioned, all three objective functions are in conflict, and it is impossible to find a solution to have optimal operational cost, ENS and VSI simultaneously. Therefore, the best strategy is to find a compromise among the three conflicted objective functions. In this regard, “Pareto optimal strategy” is applied in order to obtain a set of non-dominated solutions, and then decision makers would be able to have a tradeoff among the objective functions according to their considered priority. Fig. 7, Fig. 8 and Fig. 9 show the two-dimension Pareto optimal solutions for operational cost-ENS, operational cost-VSI and ENS-VSI, respectively. The percentages in these figures show the amount of conflict between the objective functions. The most conflict is observed in the operational cost-VSI case with 70.69%, while the minimum conflict is between ENS-VSI with 5.3%. The conflict between operational cost-ENS is 9.69%. In order to have a reliable and secure operational cost, it is better than to find a set of three-dimension non-dominated solutions.

Three-dimension Pareto front is shown in Fig. 10. The best compromise solution with the equal priority weight ($w_1 = w_2 = w_3 = 0.33$) is highlighted with a red star.

For this solution, the amounts of operational cost, ENS and VSI are \$13933.064, 373.96 kWh/year and 3.213 p.u., respectively.

The list of open switches for best compromise solution is listed in TABLE IV. According to these results, the crucial constraint for the radial structure is satisfied for each topology. Furthermore, Fig. 11 and Fig. 12 depict the active power output of diesel generators and active power of charging/discharging of batteries, respectively. From Fig. 11, it can be observed that the diesel generators are operated close to their middle levels in order to have a secure and reliable operation plan.

According to the energy not supplied formulation, it is better to feed the load consumption locally instead of feeding them through the transmission system. Then with respect to ENS improvement, the diesel generators tend to operate at their maximum level to feed the load consumption locally. The same analysis can be done for VSI. In order to increase the distribution load-ability, it is better to feed the load consumption locally. In the other way, diesel generators tend to operate at their minimum level in order to minimize the operational cost, and then the best compromise makes a tradeoff between these two different tendencies.

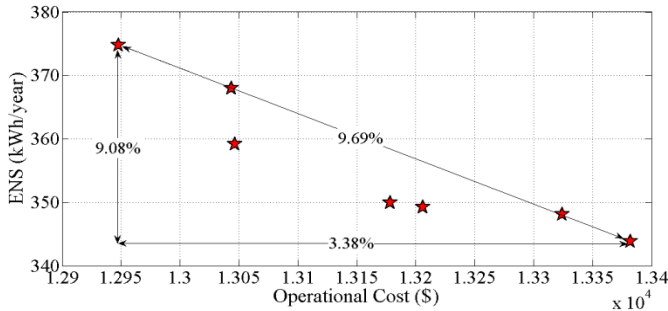


Fig. 7. Two-dimension Pareto front for operational cost-EENS

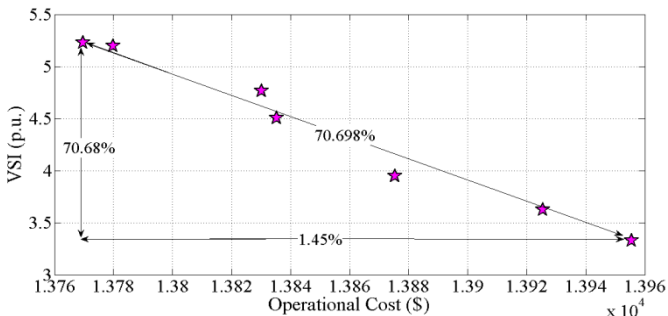


Fig. 8. Two-dimension Pareto front for operational cost-VSI

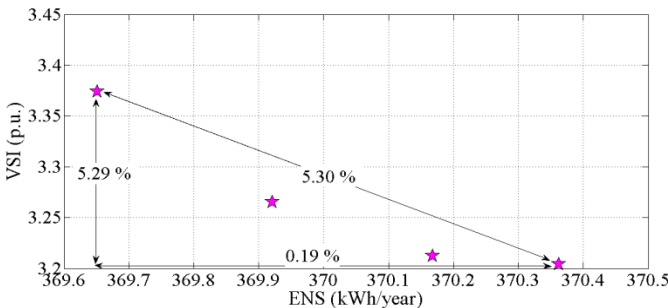


Fig. 9. Two-dimension Pareto front for EENS-VSI

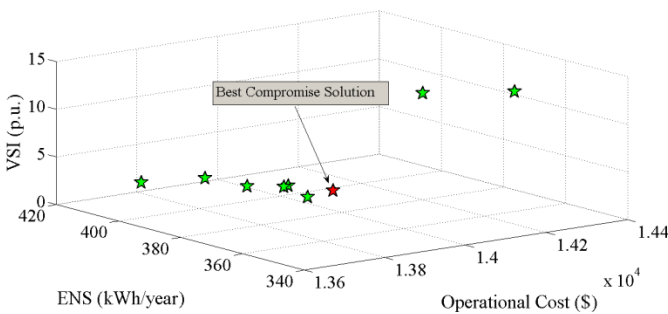


Fig. 10. Three-dimension Pareto front for operational cost-ENS-VSI

3) *Unbalanced case study*: In this subsection, the proposed approach is tested on an unbalanced version of the 119-bus distribution network. Compared to the original balanced test case, the total loads are 22654 kW and 16980 kVar at phase A, 21568 kW and 16038 kVar at phase B, and 21646 kW and 16106 kVar at phase C. Furthermore, three voltage regulators are encompassed on the three main feeders. In this case, the tap positions are considered in the decision variables and optimized with the other variables simultaneously.

TABLE V shows the extracted results for individual objective as well as the multi-objective case. According to these results, the amount of operational cost and ENS are almost tripled in comparison with the single-line case study.

TABLE IV
LIST OF OPEN SWITCHES FOR BEST COMPROMISE

Hour	Open Switches
1	40- 14- 22- 49- 47- 60- 27- 56- 65- 73- 128- 129- 104- 114- 30
2	118- 24- 7- 52- 122- 58- 39- 125- 66- 87- 76- 106- 104- 113- 30
3	45- 25- 6- 121- 122- 36- 27- 57- 70- 73- 98- 105- 85- 113- 33
4	44- 25- 7- 52- 47- 36- 37- 56- 71- 87- 128- 129- 103- 131- 31
5	44- 12- 21- 50- 48- 59- 38- 57- 69- 127- 76- 105- 130- 108- 32
6	45- 119- 23- 49- 122- 36- 124- 125- 70- 73- 98- 106- 103- 117- 32
7	118- 13- 21- 121- 122- 35- 124- 55- 90- 86- 128- 129- 103- 114- 33
8	40- 10- 18- 121- 46- 36- 38- 57- 70- 74- 97- 129- 101- 114- 33
9	44- 24- 4- 53- 48- 59- 38- 125- 70- 73- 96- 129- 104- 114- 34
10	41- 13- 7- 49- 122- 58- 38- 56- 69- 86- 75- 129- 130- 116- 132
11	41- 16- 20- 53- 122- 60- 124- 54- 89- 74- 97- 129- 101- 115- 31
12	43- 25- 3- 51- 48- 61- 37- 57- 90- 74- 96- 106- 101- 117- 34
13	118- 11- 21- 49- 46- 60- 38- 54- 65- 74- 98- 80- 100- 117- 30
14	42- 15- 19- 53- 48- 36- 37- 54- 69- 74- 128- 81- 85- 115- 132
15	42- 14- 23- 51- 46- 59- 37- 57- 66- 127- 98- 81- 101- 116- 30
16	44- 25- 18- 51- 47- 61- 27- 56- 88- 74- 96- 82- 101- 108- 33
17	43- 26- 21- 49- 47- 123- 37- 125- 126- 87- 76- 82- 130- 115- 33
18	42- 14- 20- 53- 48- 36- 39- 55- 69- 87- 76- 129- 130- 116- 32
19	118- 13- 23- 52- 47- 36- 37- 57- 68- 74- 128- 106- 100- 109- 132
20	44- 11- 19- 53- 47- 58- 124- 55- 69- 127- 76- 82- 85- 117- 34
21	118- 119- 7- 49- 48- 123- 39- 57- 69- 87- 98- 106- 104- 117- 32
22	118- 26- 18- 52- 47- 59- 38- 54- 70- 127- 96- 82- 103- 108- 32
23	41- 24- 6- 53- 122- 35- 27- 54- 65- 73- 128- 106- 103- 109- 30
24	42- 119- 120- 53- 48- 59- 124- 56- 65- 127- 98- 107- 101- 131- 132

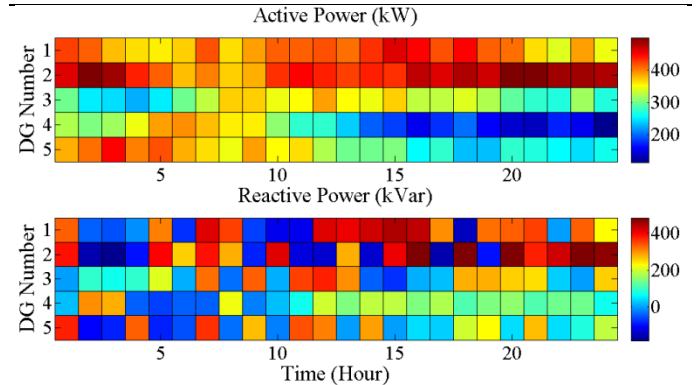


Fig. 11. The diesel generator power scheduling for the best compromise

While, the amount of VSI represents the amount of desire voltage stability index for the bus with the lowest stability margin. Furthermore, the conflict between the objective functions is obvious in the unbalanced case as well as the single-line case, and the best compromised solution provides the trade-off between the objective functions.

The list of open-switches and the tap-changer positions are tabulated in TABLE VI. In accordance with these results, it is worthwhile to note that the crucial radial constraint is satisfied at all time intervals. Moreover, it is evident that the load profile is followed by the tap-positions. In other words, during the peak load period, the tap-positions tend to increase the voltage magnitude for two reasons; the first reason is to

TABLE V
RESULTS OF OPTIMIZATION FOR THE UNBALANCED CASE

Method	Cost (\$)	ENS (kWh/year)	VSI (p.u.)
Cost Minimization	37118.89	1088.581	3.1539
ENS Minimization	38118.83	1073.687	6.0478
VSI Minimization	37578.26	1153.294	2.7322
Best Compromise	37175.70	1092.425	3.1532

TABLE VI
OPEN SWITCHES AND TAP CHANGER POSITION FOR THE BEST COMPROMISE

Hour	Open Switches	Tap Position
1	44, 24, 19, 51, 122, 58, 39, 55, 89, 74, 97, 107, 100, 115, 30	(-13), (-15), (-12)
2	40, 11, 6, 49, 122, 35, 124, 54, 67, 74, 75, 107, 104, 115, 34	(-15), (-7), (-10)
3	118, 14, 18, 53, 122, 58, 37, 57, 71, 74, 75, 105, 100, 109, 132	(-12), (-12), (-16)
4	43, 24, 22, 51, 122, 36, 27, 57, 66, 127, 96, 105, 102, 117, 132	(-12), (-15), (-10)
5	40, 14, 6, 52, 46, 123, 124, 57, 67, 127, 76, 82, 104, 117, 31	(-9), (-15), (-14)
6	44, 13, 17, 53, 46, 35, 39, 56, 90, 86, 97, 82, 103, 109, 32	(3), (10), (11)
7	42, 11, 20, 49, 46, 123, 37, 55, 68, 74, 76, 82, 101, 113, 30	(15), (14), (14)
8	43, 16, 19, 51, 48, 58, 37, 57, 67, 87, 128, 81, 104, 116, 132	(-8), (-14), (-16)
9	45, 15, 18, 53, 122, 59, 38, 125, 88, 127, 98, 80, 104, 117, 33	(-7), (-8), (-15)
10	42, 15, 20, 121, 122, 60, 37, 56, 70, 86, 98, 106, 100, 131, 32	(-16), (-10), (-14)
11	42, 11, 7, 52, 47, 35, 39, 125, 88, 87, 75, 82, 104, 115, 30	(-8), (-11), (-10)
12	40, 15, 23, 49, 122, 35, 39, 125, 69, 127, 76, 82, 130, 116, 132	(10), (10), (9)
13	118, 16, 21, 50, 47, 60, 39, 57, 71, 74, 96, 82, 103, 109, 30	(10), (9), (8)
14	43, 26, 23, 52, 122, 35, 38, 57, 68, 74, 98, 81, 102, 109, 31	(10), (11), (9)
15	45, 10, 19, 50, 46, 36, 124, 57, 72, 74, 97, 105, 130, 116, 30	(14), (10), (8)
16	41, 26, 120, 50, 122, 36, 38, 54, 66, 73, 98, 81, 85, 131, 132	(14), (11), (10)
17	44, 16, 18, 53, 122, 36, 39, 125, 69, 73, 97, 80, 104, 114, 33	(15), (16), (13)
18	118, 14, 19, 52, 48, 60, 124, 57, 89, 86, 128, 80, 85, 116, 34	(15), (16), (14)
19	40, 26, 17, 53, 47, 58, 124, 54, 90, 87, 75, 106, 104, 114, 30	(15), (16), (14)
20	40, 13, 18, 49, 46, 58, 38, 57, 88, 73, 97, 80, 130, 109, 33	(-1), (3), (-2)
21	41, 11, 23, 49, 122, 36, 37, 54, 88, 87, 98, 81, 85, 113, 33	(-1), (-1), (-2)
22	44, 15, 120, 53, 48, 35, 27, 56, 126, 74, 75, 129, 130, 131, 33	(-3), (-2), (-2)
23	43, 24, 21, 53, 46, 35, 39, 54, 70, 127, 98, 107, 101, 114, 34	(-4), (-5), (-4)
24	45, 13, 21, 53, 46, 59, 38, 57, 69, 73, 76, 106, 101, 116, 33	(-5), (-7), (-9)

avoid voltage drop, and the second one is to decrease power losses. In the off-peak period, the tap changers will reduce the voltage magnitude in order to avoid the over-voltage issue. The total energy transaction of batteries during their charge and discharge and the average active and reactive power of DGs are listed in 0. The results indicate that the batteries at buses 31 and 109 have more penetration in comparison with the batteries located at buses 42 and 96.

TABLE VII
THE PENETRATION OF BATTERIES AND DGs IN THE UNBALANCED

Batteries Energy Transaction					
Battery No.	Bus# 31	Bus# 42	Bus# 96	Bus# 109	
E (kWh)	1002.3	751.3	399.6	1190.6	
The Average DGs Power Transaction					
DG No.	Bus# 20	Bus# 28	Bus# 71	Bus# 74	Bus# 111
P (kW)	468.92	413.93	432.425	248.16	418.98
Q (kVar)	167.12	135.55	181.84	92.54	136.05

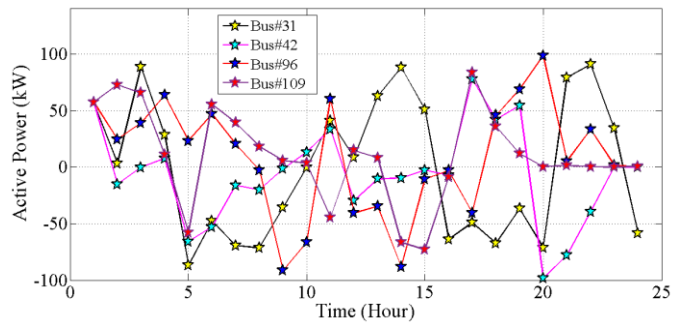


Fig. 12. Active power of batteries during charge and discharge for the best compromise

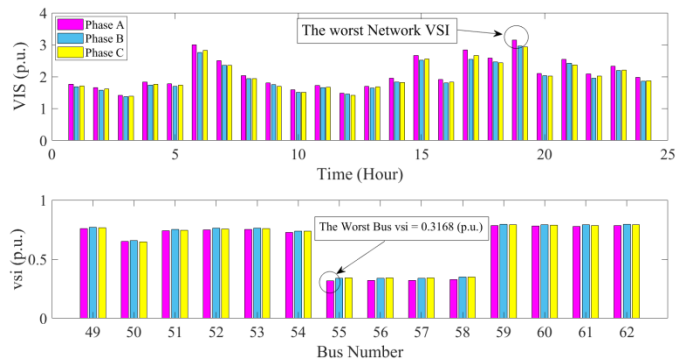


Fig. 13. Distribution network VSI profile (upper), distribution network bus-vsi profile at hour #19 (lower)

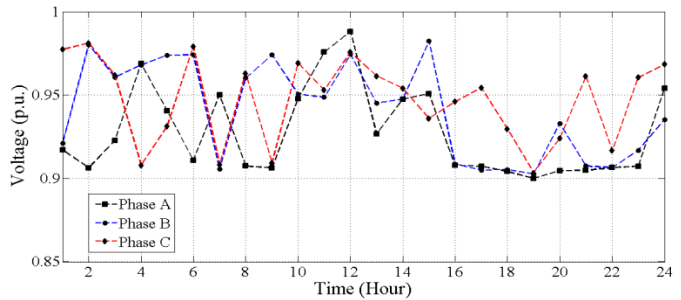


Fig. 14. Daily voltage profile for bus 55

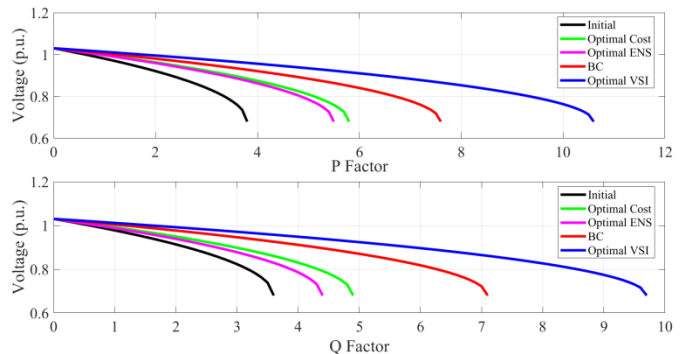


Fig. 15. P-V and Q-V curves of bus 55 as the result of load variations

Also, the results depict that the DGs at buses 20 and 74 have the most and the least commitment in the distribution network, respectively. The DGs at buses 28, 71 and 111 have approximately the same commitment with a value less than the DG at bus 28.

Aiming to have a better understanding of the improvement in terms of VSI based on distribution network loadability, some analysis is performed as follows.

Error! Reference source not found. Fig. 13 (upper) shows the network voltage stability profile during the 24-hour time horizon. According to this figure, the worst voltage stability happens at hour #19. Furthermore, the bus-vsi profile at hour #19 and the worst bus-vsi are shown in Fig. 13 (lower)**Error! Reference source not found.** The worst bus-vsi happens at the bus 55 with 0.31684 p.u., and the daily voltage profile of this bus is depicted in Fig. 14. The P-V and Q-V curves for presented strategies are plotted in Fig. 15. The continuous-power-flow method is used to plot these curves for the weakest bus at the critical hour (19 o'clock) in the case study. Obviously, by improving the VSI, the stability margin is increased.

IV. CONCLUSION

This paper proposed a new energy management strategy in dynamic distribution network reconfiguration considering renewable energy resources and energy storage to improve the distribution network security and reliability besides minimizing operational cost. The simulation results showed that the proposed strategy obtained the reasonable and high-quality schedules for switching, batteries charging and discharging, and the active power values of diesel generators in both single-objective and multi-objective frameworks. Furthermore, the exact energy not supplied index and voltage stability index as separate objective functions are considered to have an optimal operation in a reliable and secure environment. Numerical results for various cases were performed to demonstrate the ability of the proposed strategy in achieving the optimal solutions from the perspective of the DISCO. The proposed distribution network voltage stability assessment using PV and QV curves analysis distinguished the proposed study from other studies in this area.

V. REFERENCES

- [1] E. Dall'Anese, S. V. Dhople, and G. B. Giannakis, "Optimal dispatch of photovoltaic inverters in residential distribution systems," *IEEE Transactions on Sustainable Energy*, vol. 5, no. 2, pp. 487-497, 2014.
- [2] A. Azizivahed, E. Naderi, H. Narimani, M. Fathi, and M. R. Narimani, "A new bi-objective approach to energy management in distribution networks with energy storage systems," *IEEE Transactions on Sustainable Energy*, vol. 9, no. 1, pp. 56-64, 2018.
- [3] R. Li, W. Wang, and M. Xia, "Cooperative planning of active distribution system with renewable energy sources and energy storage systems," *IEEE Access*, vol. 6, pp. 5916-5926, 2018.
- [4] W. Yi, Y. Zhang, Z. Zhao, and Y. Huang, "Multiobjective Robust Scheduling for Smart Distribution Grids: Considering Renewable Energy and Demand Response Uncertainty," *IEEE Access*, vol. 6, pp. 45715-45724, 2018.
- [5] M. R. Narimani, A. A. Vahed, R. Azizpanah-Abarghoee, and M. Javidsharifi, "Enhanced gravitational search algorithm for multi-objective distribution feeder reconfiguration considering reliability, loss and operational cost," *IET Generation, Transmission & Distribution*, vol. 8, no. 1, pp. 55-69, 2014.
- [6] Q. Peng, Y. Tang, and S. H. Low, "Feeder reconfiguration in distribution networks based on convex relaxation of OPF," *IEEE Transactions on Power Systems*, vol. 30, no. 4, pp. 1793-1804, 2015.
- [7] E. Mahboubi-Moghaddam, M. R. Narimani, M. H. Khooban, and A. Azizivahed, "Multi-objective distribution feeder reconfiguration to improve transient stability, and minimize power loss and operation cost using an enhanced evolutionary algorithm at the presence of distributed generations," *International Journal of Electrical Power & Energy Systems*, vol. 76, pp. 35-43, 2016.
- [8] T. Niknam, E. Azadfarani, and M. Jabbari, "A new hybrid evolutionary algorithm based on new fuzzy adaptive PSO and NM algorithms for distribution feeder reconfiguration," *Energy Conversion and Management*, vol. 54, no. 1, pp. 7-16, 2012.
- [9] M. Abdelaziz, "Distribution network reconfiguration using a genetic algorithm with varying population size," *Electric Power Systems Research*, vol. 142, pp. 9-11, 2017.
- [10] M. Nick, R. Cherkaoui, and M. Paolone, "Optimal Planning of Distributed Energy Storage Systems in Active Distribution Networks Embedding Grid Reconfiguration," *IEEE Transactions on Power Systems*, 2017.
- [11] A. Azizivahed, E. Naderi, H. Narimani, M. Fathi, and M. R. Narimani, "A New Bi-Objective Approach to Energy Management in Distribution Networks with Energy Storage Systems," *IEEE Transactions on Sustainable Energy*, 2017.
- [12] S. R. Deeba, R. Sharma, T. K. Saha, D. Chakraborty, and A. Thomas, "Evaluation of technical and financial benefits of battery-based energy storage systems in distribution networks," *IET Renewable Power Generation*, vol. 10, no. 8, pp. 1149-1160, 2016.
- [13] M. Falahi, S. Lottifard, M. Ehsani, and K. Butler-Purry, "Dynamic model predictive-based energy management of DG integrated distribution systems," *IEEE Transactions on Power Delivery*, vol. 28, no. 4, pp. 2217-2227, 2013.
- [14] K. Khawaja, S. U. Khan, S.-J. Lee, Z. M. Haider, M. K. Rafique, and C.-H. Kim, "Optimal sizing and allocation of battery energy storage systems with wind and solar power DGs in a distribution network for voltage regulation considering the lifespan of batteries," *IET Renewable Power Generation*, 2017.
- [15] B. Lin and W. Wu, "Economic viability of battery energy storage and grid strategy: A special case of China electricity market," *Energy*, vol. 124, pp. 423-434, 2017.
- [16] Z. Li, S. Jazebi, and F. De León, "Determination of the optimal switching frequency for distribution system reconfiguration," *IEEE Transactions on Power Delivery*, vol. 32, no. 4, pp. 2060-2069, 2017.
- [17] F. Ding and K. A. Loparo, "Feeder reconfiguration for unbalanced distribution systems with distributed generation: a hierarchical decentralized approach," *IEEE Trans. Power Syst.*, vol. 31, no. 2, pp. 1633-1642, 2016.
- [18] H. Khazaei, B. Vahidi, S. H. Hosseinian, and H. Rastegar, "Two-level decision-making model for a distribution company in day-ahead market," *IET Generation, Transmission & Distribution*, vol. 9, no. 12, pp. 1308-1315, 2015.
- [19] R. Billinton and R. N. Allan, *Reliability evaluation of engineering systems*. Springer, 1992.
- [20] M. Gitizadeh, A. A. Vahed, and J. Aghaei, "Multistage distribution system expansion planning considering distributed generation using hybrid evolutionary algorithms," *Applied energy*, vol. 101, pp. 655-666, 2013.
- [21] D. A. Bell, *Fundamentals of Electric Circuits: Lab Manual*. Oxford University Press, Inc., 2009.
- [22] M. Chakravorty and D. Das, "Voltage stability analysis of radial distribution networks," *International Journal of Electrical Power & Energy Systems*, vol. 23, no. 2, pp. 129-135, 2001.
- [23] J. Aghaei, K. M. Muttaqi, A. Azizivahed, and M. Gitizadeh, "Distribution expansion planning considering reliability and security of energy using modified PSO (Particle Swarm Optimization) algorithm," *Energy*, vol. 65, pp. 398-411, 2014.

- [24] M. Barani, J. Aghaei, M. A. Akbari, T. Niknam, H. Farahmand, and M. Korpás, "Optimal Partitioning of Smart Distribution Systems into Supply-Sufficient Microgrids," *IEEE Transactions on Smart Grid*, 2018.
- [25] A. J. Conejo, F. J. Nogales, and J. M. Arroyo, "Price-taker bidding strategy under price uncertainty," *IEEE Transactions on Power Systems*, vol. 17, no. 4, pp. 1081-1088, 2002.
- [26] T. Niknam, M. Zare, and J. Aghaei, "Scenario-based multiobjective volt/var control in distribution networks including renewable energy sources," *IEEE Transactions on Power Delivery*, vol. 27, no. 4, pp. 2004-2019, 2012.
- [27] L. Wu, M. Shahidehpour, and T. Li, "Stochastic security-constrained unit commitment," *IEEE Transactions on Power Systems*, vol. 22, no. 2, pp. 800-811, 2007.
- [28] M. M. Eusuff and K. E. Lansey, "Optimization of water distribution network design using the shuffled frog leaping algorithm," *Journal of Water Resources planning and management*, vol. 129, no. 3, pp. 210-225, 2003.
- [29] D. Zhang, Z. Fu, and L. Zhang, "An improved TS algorithm for loss-minimum reconfiguration in large-scale distribution systems," *Electric Power Systems Research*, vol. 77, no. 5-6, pp. 685-694, 2007.